

Polarisation in CSS/GPS radio sources

D. Dallacasa^{1,2}

¹ Dipartimento di Astronomia, Università di Bologna, via Ranzani 1, I-40127, Bologna, Italy

² Ist. di Radioastronomia – CNR, via Gobetti 101, I-40129, Bologna, Italy

Abstract. The polarisation properties of the intrinsically small (< 20 kpc) radio sources are briefly discussed. At centimetric and decimetric wavelengths, substantial polarised emission is often detected in quasars and, at a lower level, in radio sources identified with galaxies with projected linear sizes in excess of a few kpc. The projected linear size at which some polarised emission is detected decreases with observing frequency.

High Rotation Measures are commonly found in these sources, implying high electron/ion densities and/or strong interstellar magnetic fields. For the objects found unpolarized at resolutions of the order of a few pc, either the source magnetic field is highly disordered or the scale of ambient magnetic field cells is not resolved.

1. Introduction

1.1. On CSS/GPS radio sources

Compact Steep-Spectrum (CSS) and GHz Peaked-Spectrum (GPS) radio sources are powerful ($P_{1.4\text{GHz}} > 10^{25}$ W/Hz) extragalactic objects characterized by a small physical size (typically $\leq 20 h^{-1}$ kpc¹ and $\leq 1 h^{-1}$ kpc, respectively for CSSs and GPSs). Their optically thin radio emission has a steep spectrum ($\alpha > 0.5$, $S \sim \nu^{-\alpha}$) and turns over around hundreds of MHz (CSSs) or around 1 GHz (GPSs).

They represent a significant fraction ($\simeq 15\text{--}30\%$) of the radio source population at cm wavelengths and are generally associated with distant objects ($z > 0.2$), both galaxies and quasars. The fraction of quasars increases with flux density and peak frequency, and reaches about 50% in bright CSS and GPS samples (see below). Given that quasars are generally found at a higher redshift than galaxies, the intrinsic peak frequency is higher in quasars than in galaxies (see O’Dea 1998).

It is believed that at least those with two-sided radio emission represent the young stage in the radio source evolution, from Compact (size $< 1 h^{-1}$ kpc) to Large (size $> 20 h^{-1}$ kpc) Symmetric Objects (Fanti et al. 1995; Readhead et al. 1996; Snellen et al. 2000, 2003). The measurements of hot-spot proper motions in Compact Symmetric Objects (CSO) characterised by projected linear sizes of the order of a few hundreds pc (Polatidis & Conway 2003) and with separation velocities of the outer edges of $\sim 0.1\text{--}0.4 h^{-1} c$, imply kinematic ages of the order of than 3×10^3 years or even less for the smallest objects. Among the sources considered by Polatidis & Conway, ten have proper motion detected in excess of $0.1c$, while three have upper limits to the separation speed between 0.05 and $0.1c$.

On the other hand, the spectral ages, based on synchrotron ageing arguments and pinpointed by a break in

the total radio spectrum, are of the order of $10^3\text{--}10^5$ years for the sources studied in Murgia et al. (1999) and Murgia (2003), in very good agreement with kinematic ages derived for the objects in common with Polatidis & Conway (2003). All these findings support the “youth” scenario, against the idea of “frustration” (e.g. Baum et al. 1990), requiring a particularly dense ambient medium capable of preventing the source growth and then confining the radio emission to subgalactic size for its whole lifetime.

1.2. On polarisation properties

Synchrotron radiation is intrinsically **linearly** polarised since each electron is forced to oscillate on a plane perpendicular to the local magnetic field lines. In general, if linearly polarised radiation crosses an external region where magnetic field and free electrons coexist, the orientation of the intrinsic polarisation vector is rotated by:

$$\Delta\theta \sim \text{RM} \times \lambda^2 \quad (\text{rad})$$

where RM stands for Rotation Measure:

$$\text{RM} = 812 \int_l n_e B_{\parallel} dl \quad (\text{rad/m}^2)$$

where B_{\parallel} is the field component along the line of sight. This effect takes place inside the radio source itself, or may happen along the path traveled by the polarised radiation.

An ensemble of electrons in a perfectly ordered magnetic field may emit radiation linearly polarised up to 70% since we have to consider that the photons emitted at distances larger than the surface of the volume filled in by the radio source itself must travel in a region where the source magnetic field and the ions (electrons) rotate the polarisation plane. The presence of hot (i.e. ionised) thermal plasma within the volume of the radio source may depolarise the radiation in a manner extremely difficult to predict.

¹ $H_0 = 100h \text{ km s}^{-1} \text{ Mpc}^{-1}$ and $q_0 = 0.5$ have been assumed.

On the contrary, if a Faraday screen is located along the line of sight, the behaviour of the polarised emission strongly depends on the geometry and on the characteristic scale of the magnetic field fluctuations. If the cells (i.e. regions where the field can be considered uniform) of this Faraday screen are not resolved by the observation the observed fractional polarisation can be reduced to a much lower level and even down to zero, given that differential rotation within the beam may produce a null average of the polarisation vectors, one for each cell (beam depolarisation).

Otherwise, a partially/fully disordered magnetic field within the radio source may largely reduce the fractional polarisation, and even completely depolarise the radiation leaving the radio source.

Fractional polarisation close to the theoretical maximum (70%) have been found in relaxed regions of extended radio sources, i.e. in the radio lobes and backflow tails, on scales of tens of kpc. On smaller scales, relevant to CSS/GPS radio sources, instead, such values have never been observed.

In general, bright CSS/GPS sources are known to possess either little or no linearly polarised emission, with a few outstanding exceptions (quasar only) which will be briefly discussed further down.

No circular polarisation (CP) has ever been detected at a fraction of a % level in CSS/GPS sources. Indeed CP is detected in the cores or at the jet base in some blazars, i.e. sources where relativistic beaming plays a major role. It is well known instead that such effect is negligible in CSS/GPS sources.

Given their small linear size, it is clear that the interstellar medium of the host galaxy acts as main Faraday screen on the linearly polarised emission, since the dominant contribution to the intervening column density generally comes from the radio source host. As previously stated, if the characteristic scale of the “inhomogeneities” in this medium is not resolved by the observations then the beam depolarisation can reduce the degree of polarisation, even down to zero.

Further, since the jets of the radio source are still digging their way within the host galaxy, they could induce shocks into the ISM producing a cocoon of ionised material surrounding the working surface of the radio source (Bicknell et al. 1997). This is more relevant within the NLR where the density is larger and there are plenty of clouds of ionised material.

VLA observations at cm wavelengths have demonstrated that some CSS sources possess high integrated RM (Taylor et al. 1992), in the range of the thousands rad/m^2 . The only other radio sources with comparably high RM values are found at the center of rich clusters of galaxies where high electron/ion densities (the very hot intergalactic gas responsible for the diffuse X-ray emission) and intergalactic magnetic fields around $10 \mu\text{G}$ can be found. The typical tangling scale of this screen is between 1-100 kpc.

It is expected to be much smaller in the region surround-

ing CSS/GPS radio sources, and this, in turn, would imply a substantial beam depolarisation. High frequency (tens of GHz) polarisation observations with pc-scale resolution are therefore a very important tool to study the linear polarisation in intrinsically small sources.

Lobe asymmetries coupled to polarisation information may be of great importance in the study of the role played by jet/ambient interaction, since the (more) polarised side is expected to trace the approaching side of the radio source, which is expected to be slightly brighter and larger (and at a greater distance to the core) with respect to the receding side, in standard source models.

2. Samples of CSS/GPS radio sources

The historical samples of intrinsically small radio sources have selected the brightest objects of this class (the CSSs in Fanti et al. 1990; the GPSs in Stanghellini et al. 1998; we can also include the High Frequency Peakers - HFPs - in Dallacasa et al. 2000, namely radio sources with spectra peaking at frequencies higher than a few GHz). In these bright samples the fraction of sources identified with quasars is around 50% with a tendency to increase with peak frequency. Going to lower flux densities the quasar fraction decreases progressively (Snellen et al. 1998; Marecki et al. 1999; Fanti et al. 2001) indication of a less extreme population.

If we refer to the Unified Scheme model (e.g. Urry and Padovani 1995), CSS/GPS galaxies have the jet axis close to the plane of the sky, while the CSS/GPS quasars are at intermediate angles; small sources with the jet axis close to the line of sight would appear as flat spectrum radio quasars. Therefore it is expected that the projected linear size in radio quasars is somehow shortened by projection effects, although the radio steep spectrum and a general stability of the flux density ensure that relativistic beaming have marginal effects in the vast majority of the CSS quasars.

Some support to this picture comes from the radio morphologies of CSS/GPS radio sources, observed at kpc resolution with the VLA (and MERLIN) and at pc resolution with VLBI. The radio emission in galaxies is dominated by mini-lobes. They often hosts more compact structures which can be considered as hot-spots given that their local spectrum is well fitted by a power-law (Orienti et al. 2004; Murgia et al. in preparation). Cores are generally weak and often remain undetected. In a few cases also jets are visible. The radio emission in CSS/GPS quasars is instead characterised either by jets as a whole or by individual knots. These jets sometimes show bends and contribute to most of the total source luminosity. Cores are detected more frequently than in CSS/GPS galaxies and have a larger contribution (but still at a few % level) to the source total flux density, although there are very few rare cases where the core is the most luminous component. These morphological properties are in agreement with the expectations from the Unified Scheme models.

Studies on the forementioned samples have led to build the following paradigm to describe the polarisation properties of CSS/GPS sources:

1. Galaxies are generally unpolarized or, at least, strongly depolarised
2. Quasars are either highly polarised (up to $\sim 10\%$) or completely depolarised
3. High RM (exceeding 1000 rad/m^2) are generally found in CSS/GPS sources
4. Polarisation and flux density variability are not common in CSS/GPS radio sources

3. Integrated linear polarisation

One of the characteristics of CSS/GPS galaxies is the very low or even absent linear polarisation at cm wavelengths. This property can be related to the source growth model and then relates the observed polarisation to the projected linear size, that is, in turn, related to the turnover frequency (see e.g. O’Dea 1998). Based on the work of Stanghellini et al. (1998), it is clear that GPS galaxies have upper limits of 0.3% (but many as low as 0.1%) to the integrated fractional polarisation at 4.9 and 8.5 GHz. The only object (B1323+321) detected in their polarimetric VLA observations also belong to the CSS sample of Fanti et al. (1990). GPS quasars are generally weakly polarised, around 1% level, and about one third is completely unpolarised. A systematic work on the polarisation of CSS sources of Fanti et al. (1990) has not been carried out. We can refer to van Breugel et al. (1984;1992) and Lüdke et al. (1998) to find out that CSS galaxies are weakly polarised if not at all; CSS quasars instead have outstanding sources for which cases of percentage of polarisation as high as 10% are observed even at decimetric wavelengths. A few examples will be discussed further down. A number of these CSS quasars are used as calibration sources for both flux density and absolute orientation of the electric vector of the linear polarisation. A requirement for such use is to have a **stable** flux density and polarisation (in both intensity and orientation of the electric vector), which can be considered a quite unusual characteristic if compared to what is seen flat spectrum radio quasars and BL Lacs, in which both quantities may vary substantially (Cawthorne et al. 1993). This can be considered a further evidence for the different nature of CSS quasars, in which cores and components at the jet base little contribute at the total source flux density and polarisation,.

An interesting view has been given by Cotton et al. (2003a) and Fanti et al. (2004) who studied the B3-VLA CSS sources sample (Fanti et al. 2001). These are sources with radio luminosities generally lower than in the Fanti et al. (1990), and the fraction of galaxies (or empty fields) is much larger. By using the NVSS data, Cotton et al. (2003a) found that at 20 cm all sources with projected linear size smaller than 6 kpc are not polarised; part of the larger sources instead show some amount of polarisation. The analysis of VLA A-configuration data presented

by Fanti et al. (2004) at 6 and 3.6 cm (see their Fig. 8) demonstrates that the cutoff, quite sharp at 20 cm, moves inward the radio source and becomes shallower at progressively shorter wavelengths. In particular, at 3.6 cm the median level of polarisation is 4% for the sources with projected linear size exceeding 5 kpc. For many of these sources with substantial polarisation even in the NVSS, it is possible to study the RM: only about 50% of the sources follow the expected λ^2 law, and this might be due to a complex field geometry and/or differential effects within the radio source. Only about 20% of the sources have intrinsic rotation measure exceeding 1000 rad/m^2 , and in these cases the depolarisation gets substantial at lower frequencies (Fanti et al. 2004).

4. Parsec scale polarisation

A possibility to attribute polarised emission to the smallest CSS/GPS sources despite their low or absent integrated linear polarisation is to invoke beam depolarisation.

A viable method to investigate this possibility consists of very high resolution observations capable to resolve Faraday screen with scales of the order of a few parsec. This implies the use of VLBI.

4.1. Galaxies

As already mentioned, the integrated linear polarisation in CSS/GPS/HFP sources identified with galaxies is generally consistent with being 0.0% at dm and even at cm wavelengths. Indeed, the absence of linear polarisation can be used also as a tool to distinguish small and young radio sources from flat spectrum compact radio sources when observed at arcsecond resolution.

One possibility to explain such characteristic refers to a complicated magnetic field geometry implying a largely reduced integrated polarisation when averaging over vectors with globally random distribution. The same result is obtained if an ordered linearly polarised emission crosses a region of space where there is a substantial electron density and a randomly oriented magnetic field, whose characteristic structure happens to be very small, of the order of a few pc.

CSS or GPS galaxies sources like B0404+768 or B1943+546 are unpolarised in VLA observations at cm wavelengths. Their angular size are about 150 and 40 mas respectively, and then their study requires polarimetric VLBI observations. They have been observed in a program mainly aiming to investigate local spectral ageing in their different regions (Murgia et al. in preparation), but also polarimetry has been carried out. The images at 8.4 GHz of latter source in total intensity (IPOL) and polarised emission (PPOL) are presented in Fig. 1 and Fig. 2, respectively. The source structure (Fig. 1) consists of an unresolved core and two asymmetric lobes, whose radio emission at this frequency is dominated by the hot-spots and the beginning of backflow tails. Polarisation images

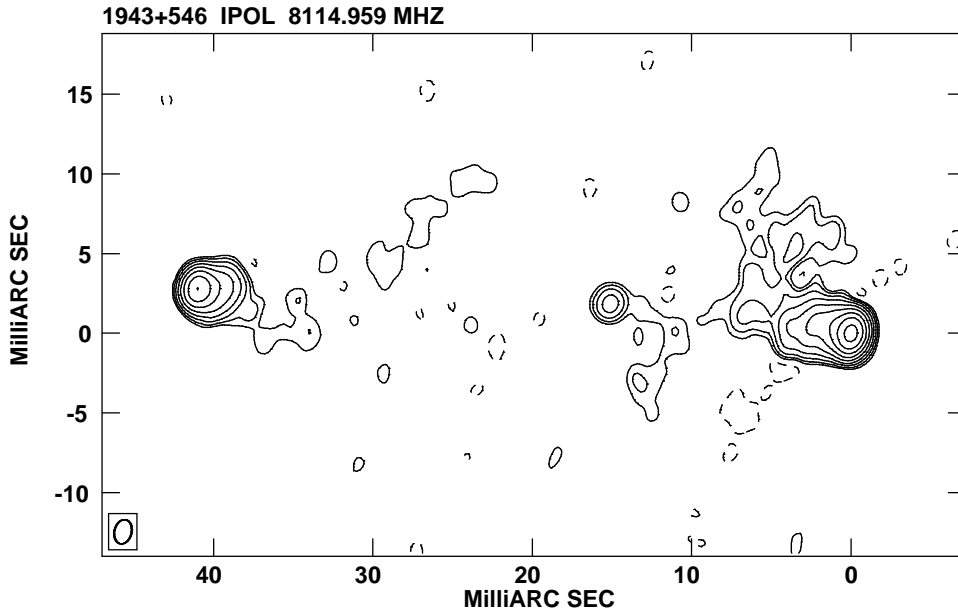


Fig. 1. Full resolution total intensity image of B1943+546. The first contour is ± 0.7 mJy/beam, and the levels scale up by a factor of 2. Some more diffuse emission from the lobes is resolved out

turned out to consist of pure noise, indication of lack of any substantial polarised emission at a level of a fraction of a mJy. The PPOL image in Fig. 2 does not show any sign of emission related to the total intensity. Also a tapered image (not shown) obtained to recover most of the flux density in the radio lobes does not show any sign of polarised emission. The local fractional polarisation has then upper limits ranging from 0.2% in the western hot-spot up to a few % in the more diffuse lobe emission, but it is likely that the intrinsic linear polarisation at this frequency is much lower.

A similar conclusion can be drawn for B0404+768: the highest frequency with polarisation images available is 5.0 GHz (not shown here; Morandi et al. in preparation): the peak in the PPOL image is less than 1 mJy at 5.0 GHz, with upper limits to the linear polarisation of about 0.4% in the South-Western hot-spot and, similarly to B1943+546, of a few percent in the regions within the lowest IPOL contour.

Similar results can be also found in a few GPS galaxies observed at 2 cm with the VLBA by Stanghellini et al. (2001). Thanks to the relatively short wavelength, some amount (at $\sim\%$ level) of linear polarisation is locally detected on the brightest regions (never in the cores), but most of the source structure appears unpolarised.

As mentioned above, it is possible to conclude that beam depolarisation is likely NOT to be the reason of the low linear polarisation seen in GPS (and smaller CSS) galaxies. Then, either the screen inhomogeneities are not resolved on scales of a few pc, or the magnetic field within

the radio source is not ordered (both possibilities may play a role at the same time).

4.2. Quasars

In this section the polarisation properties of a few, well known, CSS quasars are briefly discussed. In general they have a variety of behaviours, with no obvious link to other observed quantities like the projected linear size, turnover frequency and so on.

Famous examples are 3C48, 3C138, 3C147 and 3C286, also well known to be calibration sources for the absolute orientation of the electric vector on the sky. Further examples of well known bright CSS quasars with substantial polarised emission are 3C216 and 3C380.

A few others possess unusual polarisation properties: Lüdke et al. 1998 show that 3C190 does not have polarised emission at 6 cm in their MERLIN observation, but they quote that the fractional polarisation has been found as high as 10% in VLA data at 2 cm (van Breugel et al. 1992 implying a strong depolarisation between these two wavelengths).

3C138 is a well known quasar whose pc-scale radio structure is known since the early '80s, and whose polarisation properties have been investigated by Dallacasa et al. 1995b; Cotton et al. 1997 and 2003b. This source is particularly interesting since it shows a bright jet with polarisation of $\sim 10\%$, and a core region with a much weaker polarisation ($\sim 3\%$) where the true core and another component, likely the first knot at the beginning

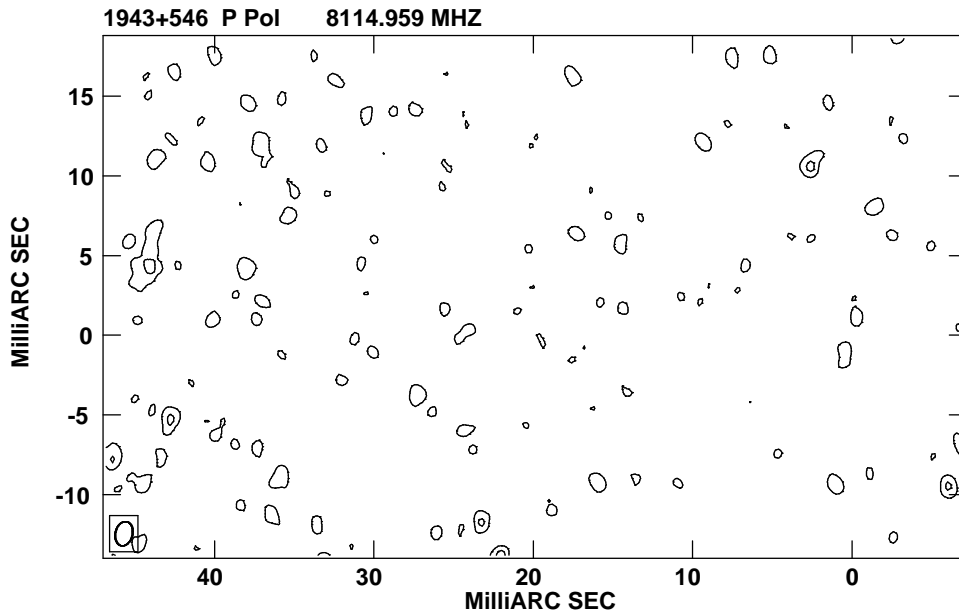


Fig. 2. Full resolution polarised emission of B1943+546. The first contour is 0.3 mJy/beam, and the levels scale up by a factor of 2. This image has been corrected for the positive bias.

of the main jet, are embedded in a diffuse emission. This knot has some linear polarisation. A monitoring program carried out with full polarisation to study the motion of this knot has provided the following evidence: the motion of the knot is at a marginal level (contrary to previous claims of superluminal motion); its polarisation properties changed in a way consistent with the possibility that the inner jet component is seen through limited holes in a dense Faraday screen.

Contrary to all this the polarisation of the main jet, the major contributor to the total polarised emission, did not show any sign of variability in both intensity or orientation of the electric vector.

Another quite famous source is 3C286: the interpretation of its structure is still matter of debate. The milliarc-second emission is dominated by a well resolved component, whose structure is similar to those seen in hot-spots in FR-II radio sources. The brightest region seen with VLBI is significantly polarised ($\sim 10\%$), and the electric vector does have a configuration resembling (again) that seen in hot spots. The polarisation angle is known to be constant at cm and dm wavelengths, and then the RM is negligible.

3C147 has total intensity morphological characteristics similar to those seen in 3C286, but the polarised emission do behave completely different. In fact substantial polarisation is detected at wavelengths shorter than 10 cm in the region with the highest brightness temperature, generally referred to as the core region. The observed RM (see Rossetti et al. these proceedings; Zhang et al 2004) reaches

about -1650 rad m^{-2} , that converts to $\sim -4000 \text{ rad m}^{-2}$ in the source frame. The polarisation of the core region is resolved into a number of individual components with RM in the range between ~ -1200 and -2400 rad m^{-2} . Once the Faraday rotation is removed, the geometry of the source magnetic field becomes similar to the one seen in 3C286 reinforcing the similarities between these two sources.

Finally, the it is worth to mention the case of OQ172. For some time in the 80's this quasar had the record for the highest redshift ($z=3.53$). The radio structure has been studied in detail by Udomprasert et al. (1997) with polarimetric VLBA observations: some amount of polarised emission arises from the jet base, in which an extremely high RM is detected and converts up to 40000 rad/m^2 in the source frame. The direction of the intrinsic magnetic field is aligned with the jet local axis.

5. Summary

The polarisation properties of the CSS/GPS sources are better seen at cm wavelengths, where depolarisation due to differential Faraday Rotation within the resolution element is less effective. Linear polarisation is not detected in GPS and in the smallest CSS galaxies. Beam depolarisations does not seem to be the reason for this, unless the Faraday screen has scales smaller than about 1 pc. Some CSS quasars appear outstanding in linearly polarised emission. Integrated fractional polarisations as high as 10% are sometimes observed over a wide range

of frequencies.

Faraday Rotation is observed in many cases, with RM in the source frame in the range between a few hundreds and a few thousands rad/m^2 , although there are also cases consistent with zero RM (e.g. 3C286) or values as high as 40000 rad/m^2 (OQ172).

Acknowledgements. Financial support from the Italian MIUR under grant COFIN-2002-02-8118 is acknowledged.

References

- Baum, S.A., O'Dea, C.P., de Bruyn, A.G., Murphy, D.W. 1990, *A&A*, 233, 379
- Bicknell, G.V., Dopita, M.A., O'Dea, C.P. 1997, *ApJ*, 485, 112
- van Breugel, W.J.M., Miley, G.K., Heckman, T. 1984, *AJ*, 89, 5
- van Breugel, W.J.M., Fanti, C., Fanti, R., Stanghellini, C., Schilizzi, R.T., Spencer, R.E. 1992, *A&A*, 256, 56
- Cawthorne, T.V., Wardle, J.F.C., Roberts, D.H., Gabuzda, D.C. 1993, *ApJ*, 416, 519
- Cotton, W.D., Dallacasa, D., Fanti, C., Fanti, R., Foley, A.R.; Schilizzi, R.T., Spencer, R.E. 1997, *A&A*, 325, 493
- Cotton, W.D., Dallacasa, D., Fanti, C., Fanti, R., Foley, A.R., Schilizzi, R.T., Spencer, R., Saikia, D.J., and Garrington, S. 2003a, *PASA*, 20, 12
- Cotton, W.D., Dallacasa, D., Fanti, C., Fanti, R., Foley, A.R., Schilizzi, R.T., Spencer, R.E. 2003b, *A&A*, 406, 43
- Dallacasa, D., Fanti, C., Fanti, R., Schilizzi, R.T., & Spencer, R.E. 1995a, *A&A*, 295, 27
- Dallacasa, D., Cotton, W.D., Fanti, C., Fanti, R., Foley, A.R.; Schilizzi, R.T., Spencer, R.E. 1995b, *A&A*, 299, 671
- Dallacasa, D., Stanghellini, C., Centonza, M., Fanti, R. 2000, *A&A*, 363, 887
- Fanti, R., Fanti, C., Schilizzi, R. T., Spencer, R. E., Nan Rendong, Parma, P., van Breugel, W. J. M., Venturi, T. 1990, *A&A*, 231, 333
- Fanti, C., Fanti, R., Dallacasa, D., Schilizzi, R.T., Spencer, R.E., & Stanghellini, C. 1995, *A&A*, 302, 317
- Fanti, C., Pozzi, F., Dallacasa, D., Fanti, R., Gregorini, L., Stanghellini, C., & Vigotti, M. 2001, *A&A*, 369, 380
- Fanti, C., Branchesi, M., Cotton, W.D., Dallacasa, D., Fanti, R., Gregorini, L., Murgia, M. et al. 2004, *A&A*, in press
- Lüdke, E., Garrington, S.T., Spencer, R.E., Akujor, C.E., Muxlow, T.W.B., Sanghera, H.S., Fanti, C. 1998, *MNRAS*, 299, 467
- Marecki, A., Falcke, H., Niezgoda, J., Garrington, S.T., Patnaik, A.R., 1999, *A&AS*, 135, 273
- Murgia, M., Fanti, C., Fanti, R., Gregorini, L., Klein, U., Mack, K.-H., & Vigotti, M. 1999, *A&A*, 345, 409
- Murgia, M. 2003, *PASA*, 20, 19
- O'Dea, C.P. 1998, *PASP*, 110, 493
- Orienti, M., Dallacasa, D., Fanti, C., Fanti, R., Tinti, S., Stanghellini, C. 2004, *A&A*, in press
- Polatidis, A.G., & Conway, J.E. 2003, *PASA*, 20, 69
- Readhead, A.C.S., Taylor, G.B., Xu, W., Pearson, T.J., Wilkinson, P.N., & Polatidis, A.G. 1996, *ApJ*, 460, 612
- Snellen, I.A.G., Schilizzi, R.T., de Bruyn, A.G., Miley, G.K., Rengelink, R.B., Roettgering, H.J., Bremer, M.N. 1998, *A&AS*, 131, 435
- Snellen, I.A.G., Schilizzi, R.T., Miley, G.K., et al. 2000, *MNRAS*, 319, 445
- Snellen, I.A.G., Mack, K.-H., Schilizzi, R. T., Tschager, W. 2003, *PASA*, 20, 38
- Stanghellini, C., O'Dea, C.P., Dallacasa, D., Baum, S.A., Fanti, R., Fanti, C. 1998, *A&AS*, 131, 303
- Stanghellini, C., Dallacasa, D., O'Dea, C.P., Baum, S.A., Fanti, R., Fanti, C. 1998, *A&A*, 377, 377
- Taylor, G.B., Inoue, M., Tabara, H. 1992, *A&A*, 264, 421
- Udomprasert, P.S., Taylor, G.B., Pearson, T.J., Roberts, D.H. 1997, *ApJ*, 483, L9
- Urry, C.M., Padovani, P. 1995, *PASP*, 107, 803
- Zhang, H.Y., Gabuzda, D.C., Nan, R.D., Jin, C.J. 2004, *A&A*, 415, 477